Unraveling the layers of cryptic genetic variation in a yeast gene regulatory network

Jonathan T. Lee*, Alessandro L.V. Coradini*†, Amy Shen*, and Ian M. Ehrenreich*

*Molecular and Computational Biology Section, Department of Biological Sciences, University of Southern California, Los Angeles, CA 90089-2910, USA

†Laboratory of Genomics and Bioenergy, Department of Genetics and Evolution, Institute of Biology, UNICAMP, Campinas, São Paulo, 13083-970, Brazil

Running title: Layers of cryptic genetic variation

Keywords: Cryptic genetic variation, epistasis, genotype-environment interaction, complex traits, genetic architecture

Corresponding author:
Ian M. Ehrenreich
Address: Molecular and Computational Biology Section, Ray R. Irani Hall 201, University of Southern California, Los Angeles, CA 90089-2910, USA
Phone #: 213 – 821 – 5349
Email: ian.ehrenreich@usc.edu

Abstract

Cryptic genetic variation may be an important contributor to heritable traits, but its extent and regulation are not fully understood. Here, we investigate the cryptic variation underlying a *Saccharomyces cerevisiae* colony phenotype that is typically suppressed in a cross. Mapping of the trait's genetic basis after induction by three different genetic perturbations identifies 21 total loci. The perturbations largely uncover distinct loci, and strongly influence additivity, epistasis, and genotype-environment interaction among these loci. Only a single locus— the coding region of the cell surface gene *FLO11*—is common to all three perturbations. While the remaining loci mostly influence *FLO11* transcription in *cis* or *trans*, we detect loci in different pathways and sub-pathways in the presence of each perturbation. Our work shows that complex gene regulatory networks can harbor multiple layers of cryptic variation, each of which may only be visible in highly specific genotypic and environmental contexts.

Article Summary

The extent and regulation of cryptic genetic variation within populations is not fully understood. To address these questions, we comprehensively dissect the genetic basis of a budding yeast colony trait following its induction by three different genetic perturbations. In total, we identify 21 distinct loci, most of which show phenotypic effects that depend on particular perturbations, other segregating loci, and temperature. We find that nearly all involved loci participate in a common gene regulatory network (GRN). Thus, our work demonstrates the large amount of cryptic variation underlying a single trait and ties the visibility of this variation to GRN activity.

Introduction

Most research on complex traits focuses on characterizing the genetic basis of phenotypic diversity that is visible within populations (ATWELL *et al.* 2010; AYLOR *et al.* 2011; MACKAY *et al.* 2012; BLOOM *et al.* 2013). Yet, these same populations can also harbor cryptic genetic variation that does not typically impact phenotype, and is only observable when particular genetic or environmental perturbations occur (RUTHERFORD AND LINDQUIST 1998; QUEITSCH *et al.* 2002; BERGMAN AND SIEGAL 2003; DWORKIN *et al.* 2003; GIBSON AND DWORKIN 2004; JAROSZ AND LINDQUIST 2010; GEILER-SAMEROTTE *et al.* 2016). This cryptic variation may be an important source of phenotypic variability in medically and evolutionarily significant traits (LE ROUZIC AND CARLBORG 2008; MCGUIGAN AND SGRO 2009; PAABY AND ROCKMAN 2014). Thus, it is imperative that we determine the extent of cryptic variation within populations, as well as the mechanisms that toggle this cryptic variation between silent and visible states. However, such work is inherently difficult because the specific perturbations needed to uncover cryptic variation, as well as the exact identities of the cryptic variants that are affected by these perturbations, are rarely known. Such information is critical to obtaining a more complete, mechanistic understanding of cryptic variation.

In previous papers, we developed an experimental system that can be used to systematically identify cryptic variants influencing a colony phenotype in *Saccharomyces cerevisiae* (TAYLOR AND EHRENREICH 2014; TAYLOR AND EHRENREICH 2015b; LEE *et al.* 2016; TAYLOR *et al.* 2016). Upon mating the lab strain BY4716 (BY) to a haploid derivative of the clinical isolate 322134S (3S), we found that BY, 3S, and nearly all of their recombinant haploid progeny form smooth colonies when grown on solid media. However, certain genetic perturbations (GPs) can enable some BYx3S segregants to express a rough colony phenotype at particular temperatures (**Figure 1A** and **1B**). Expression of the trait results from complex interactions between the GPs, segregating loci, and temperature (TAYLOR AND EHRENREICH 2014; TAYLOR AND EHRENREICH 2015b; TAYLOR AND EHRENREICH 2015a; LEE *et al.* 2016; TAYLOR *et al.* 2016). Crucially, genetic mapping and genetic engineering techniques can be used to comprehensively identify the specific cryptic variants that enable rough segregants to express the trait.

51 Our initial work on colony morphology in the BYx3S cross focused on a *de novo* loss-of-
52 function mutation in *IRA2* ('GPa'), a negative regulator of Ras signaling (TAYLOR AND
53 EHRENREICH 2014; TAYLOR AND EHRENREICH 2015b; LEE *et al.* 2016) (**Figure 1C**). Across
54 several papers, we demonstrated that GPa causes trait expression through temperature-
55 dependent, higher-order genetic interactions involving cryptic variants inherited from both BY
56 and 3S (TAYLOR AND EHRENREICH 2014; TAYLOR AND EHRENREICH 2015b; LEE *et al.* 2016).
57 Subsequently, we identified other *de novo* and introduced mutations that also facilitate
58 expression of the rough phenotype in the BYx3S cross (TAYLOR AND EHRENREICH 2015b;
59 TAYLOR *et al.* 2016). These other mutations tended to also disrupt negative regulation of
60 signaling and transcription within the Ras pathway, and mostly interacted with the same alleles
61 found in the studies focused on GPa.
62
63 In the same study, we also found that some rough BYx3S segregants lacked any detectable *de*
64 *novo* mutations (TAYLOR *et al.* 2016). Instead, the majority of these individuals inherited
65 independent recombination events within a 1.3 kb region in the promoter of the cell surface gene
66 *FLO11* ('GPb', **Figure 1D**). *FLO11* encodes a flocculin whose display on the cell surface
67 facilitates cell-cell adhesion and is required for expression of the rough phenotype (LO AND
68 DRANGINIS 1996; TAYLOR AND EHRENREICH 2015b). Genetic engineering experiments showed
69 that the recombination event brought at least two linked polymorphisms at *FLO11* onto the same
70 chromosome, resulting in a new *FLO11* haplotype that behaves like the mutations described in
71 our earlier studies (LEE *et al.* 2016). Specifically, segregants with a BY promoter and a 3S
72 coding region had the potential to express the trait. Despite discovering GPb in this past study,
73 we neither resolved the causal variant(s) in the *FLO11* promoter nor comprehensively mapped
74 the loci enabling this GP to exert a phenotypic effect. Thus, it was not possible to compare the
75 genetic basis of the rough phenotype in the presence of GPb to our initial work on GPa.
76
77 Here, we use the rough colony system to determine how different types of GPs interact with
78 distinct cryptic variants in the BYx3S cross to produce the same trait. In addition to GPa and
79 GPb, we also examine a third GP that facilitates expression of the rough phenotype. To generate
80 'GPc,' we knocked out the activator Flo8 and the repressor Sfl1, which are the main transcription
81 factors acting downstream of the Ras pathway to regulate colony morphology in the cross

82 (**Figure 1E**). Previously, we showed that deletion of *SFL1* is sufficient to enable Ras-dependent
83 cryptic variants to express *FLO11* and that transcription of *FLO11* in these *sfl1*Δ segregants is
84 Flo8-dependent (TAYLOR AND EHRENREICH 2015b). By eliminating these key regulators and
85 screening for segregants expressing the trait (**Figure 1F**), we sought to uncover previously
86 unidentified cryptic variants that can also give rise to the rough phenotype.
87
88 In this paper, we comprehensively determine the genetic basis of the rough phenotype across
89 temperatures for GPb and GPc, and compare these results to our past work on GPa. Across the
90 three GPs, we identify 21 loci that contribute to the rough phenotype. Of these loci, 20 show
91 conditional phenotypic effects that are influenced by particular combinations of GP, other loci,
92 and temperature. Although all three factors prove important, GP is by far the strongest
93 determinant of which loci show phenotypic effects, impacting nearly all identified loci. In fact,
94 12 of the detected loci only exert phenotypic effects in the presence of a single GP. Additionally,
95 we find that the identified loci exhibit varying degrees of additivity, epistasis, and genotype-
96 environment interaction depending on the GP that uncovers them. At the molecular level, most,
97 if not all, of the identified loci influence *FLO11* regulation in *cis* or *trans*, suggesting that our
98 findings result from complex genetic and environmental effects on the *FLO11* regulatory
99 network. These findings enhance our understanding of both the extent of cryptic variation within
100 populations and the mechanisms by which GPs reveal cryptic variants.
101
102 **Materials and Methods**
103 *Knockout of FLO8* and *SFL1 in BY and 3S*
104 *FLO8* and *SFL1* targeting gRNA sequences were cloned into the pML104 plasmid vector, which
105 carries Cas9 and *URA3* (LAUGHERY *et al.* 2015). Each resulting plasmid was transformed into
106 the BY and 3S strains alongside a double stranded oligo to be used as a repair template for
107 homologous recombination (HR). Two sequential knockouts were performed for each strain to
108 modify both genes. The lithium acetate method (GIETZ AND WOODS 2002) was used for
109 transformation. Repair template oligos were 90 bases long with homology to either *FLO8* or
110 *SFL1*, but with three bases replaced in frame with a stop codon to truncate the gene. A one base
111 frameshift deletion was also introduced following the stop codon to further ensure loss of gene
112 function. Stop codons were introduced at amino acid 155 and 39 in *FLO8* and *SFL1*,

113 respectively. Transformed cells were plated on solid yeast nitrogen base (YNB) media lacking
114 uracil to select for retention of the pML104 plasmid. Presence of the intended genetic
115 modifications was checked in the transformants using Sanger sequencing.
116
117 *Isolation of a rough BYx3S segregant with GPc*
118 The BY and 3S strains engineered with GPc were mated to one another. The resulting diploid
119 was sporulated and plated at low density (~300 colonies per plate) onto yeast nitrogen base
120 (YNB) agar containing canavanine to select for MATa haploids using the synthetic genetic array
121 system (TONG *et al.* 2001). After five days at 30°C, colonies were replicated onto yeast extract-
122 peptone-ethanol (YPE) plates. A single rough colony was identified after four days of growth at
123 21°C.
124
125 *Generation of backcross segregants*
126 The GPb rough segregant used in this study was obtained through a screen described in (TAYLOR
127 *et al.* 2016), in which it was referred to as 'Rough segregant 13.' To generate backcross progeny
128 for genetic mapping and segregation analysis, we mated the GPb and GPc rough segregants to
129 obtain diploids. The GPb segregant was backcrossed to wild type BY and 3S, while the GPc
130 segregant was backcrossed to *flo8*Δ *sfl1*Δ BY and 3S strains. Diploids were sporulated and plated
131 at low density onto YNB plates containing canavanine. After five days of growth at 30°C,
132 haploid colonies were replicated onto YPE plates and incubated at 21°C. Segregants expressing
133 rough morphology after four days of growth on YPE were inoculated into liquid yeast extract-
134 peptone-dextrose (YPD) media and grown overnight at 30°C. Freezer stocks of rough segregants
135 were made by mixing aliquots of these cultures with 20% glycerol solution and storing these
136 glycerol stocks at -80°C.
137
138 *Phenotyping at multiple temperatures*
139 Cells from freezer stocks were inoculated into liquid YPD media, grown for two days at 30°C,
140 and then pinned onto three YPE plates. Each plate was then incubated at a single, constant
141 temperature: 21, 30, or 37°C. The colonies were then phenotyped for expression of the colony
142 trait after four days of growth. Due to the low frequency of the rough phenotype in the GPb x 3S
143 backcross at 30 and 37°C, another round of mating was performed to enrich for individuals

144 expressing the trait in these conditions. Specifically, a 3S backcross segregant was mated to the
145 BY strain, and segregants were selected and screened for the trait in the same manner described
146 above.
147
148 *Genotyping of GPb and GPc rough segregants*
149 For each backcross, segregants expressing the rough phenotype at up to 21, 30, or 37°C were
150 inoculated into liquid YPD. DNA was extracted from overnight cultures using the Qiagen
151 DNeasy 96 Blood and Tissue kit. Illumina sequencing libraries were then prepared using the
152 Illumina Nextera kit, with a unique pair of dual-indexed barcodes for each individual. Between
153 48 and 156 segregants from each combination of GP, backcross, and temperatures sensitivity
154 were sequenced. Sequencing was performed at the Beijing Genomics Institute on an Illumina
155 HiSeq 4000 using paired-end 100x100 bp reads. Each segregant was sequenced to an average per
156 site coverage of at least 2.5x. Reads were mapped onto the S288c reference genome and a 3S
157 draft genome, from the *Saccharomyces* Genome Database, using the Burrows-Wheeler Aligner
158 (BWA) version 7 with options mem -t 20 (LI AND DURBIN 2009). SAMtools was used to
159 generate mpileup files (LI *et al.* 2009), and genome-wide allele frequencies were calculated at
160 36,756 SNPs that were previously identified between BY and 3S (TAYLOR *et al.* 2016).
161
162 *Genetic mapping of loci underlying the rough phenotype*
163 Each segregant's genotype at 36,756 SNPs was determined using a Hidden Markov model,
164 implemented in the HMM package in R. Loci associated with the trait for each combination of
165 GP, backcross, and temperature sensitivity were identified using binomial tests. Sites were
166 considered statistically significant at a Bonferroni-corrected threshold of $p < .01$. Multiple-
167 testing correction was performed on each backcross population on its own, as the number of
168 unique tests varied 837 to 1,526 among these populations. We defined the interval surrounding
169 identified loci by computing the -log10(*p*-value) at each linked SNP and determining the SNPs at
170 which this statistic was 2 lower than the peak marker for a locus. These bounds were used in
171 fine-mapping and to assess overlap among loci detected in different combinations of GP,
172 backcross, and temperature sensitivity.
173
174 *Testing for genotypic heterogeneity*

175 Observed and expected haplotype frequencies for each pair of SNPs were compared using χ^2
176 tests in a custom Python script. Expected haplotype frequencies were calculated as the product of
177 the individual allele frequencies at each of the two sites. To reduce the number of statistical tests,
178 SNPs containing the same information across all segregants in a given backcross population
179 were collapsed into a single marker. The Benjamini-Hochberg method for False Discovery Rate
180 (FDR) (BENJAMINI AND HOCHBERG 1995) was then implemented using the statsmodels Python
181 module (SEABOLD AND PERKTOLD 2010). A stringent FDR of 0.0001 was employed and regions
182 of the genome within 30,000 bases of the ends of chromosomes were excluded to avoid
183 genotyping errors.
184
185 *Exploration of additivity and epistasis*
186 Expected multi-locus genotype frequencies were calculated as the product of the frequencies of
187 the individual alleles segregating in a given backcross. For each population, observed and
188 expected genotype frequencies were compared using a χ^2 test with degrees of freedom equal to
189 one less than the number of possible genotypes. These analyses were only performed on
190 backcross populations in which three or more loci segregated.
191
192 *Genetic engineering at the FLO11 promoter and other loci*
193 Gene deletions at GP-interacting loci were accomplished by replacement with the *kanMX*
194 cassette (WACH *et al.* 1994). Using the lithium acetate transformation method (GIETZ AND
195 WOODS), a genomic region of interest was replaced with a PCR amplicon of the *kanMX* cassette
196 with 60 bases of homology to the ends of the region. Transformed cells were plated on YPD +
197 G418 to select for integration of *kanMX* and insertion was verified using PCR.
198
199 Allele replacements were performed using a two-step, CRISPR/Cas9-mediated approach. A
200 *kanMX* deletion strain, generated as described above, was transformed with the pML104 plasmid
201 (LAUGHERY *et al.* 2015) carrying the Cas9 gene and a gRNA sequence targeting *kanMX*, along
202 with a PCR product repair template that should result in excision of *kanMX* and result in an allele
203 swap. Cells were plated on YNB plates lacking uracil to select for retention of pML104.
204 Replacement of the *kanMX* cassette was verified by PCR, and transformants were plated and
205 screened on YPE to determine the phenotypic effects of allele replacement. All replacements

206 were confirmed by Sanger sequencing. Also, in parallel with each allele replacement, we
207 generated control strains where *kanMX* was replaced with the original sequence at a given site.
208 The phenotypes of allele replacement strains were assessed based on comparison to control
209 strains that had been generated in parallel.
210
211 **Results**
212 *Isolation of a rough flo8Δ sfl1Δ segregant*
213 Our past work showed that expression of the rough phenotype in the BYx3S cross mainly occurs
214 due to genetic interactions between GPs and polymorphisms in the Ras pathway (TAYLOR AND
215 EHRENREICH 2014; TAYLOR AND EHRENREICH 2015b; LEE *et al.* 2016; TAYLOR *et al.* 2016). To
216 examine whether genetic variation beyond the Ras pathway might also be able to contribute to
217 the trait, we knocked out *FLO8* and *SFL1* in both BY and 3S using CRISPR/Cas9 (**Methods**).
218 We then employed random spore techniques to generate and screen > 100,000 *flo8Δ sfl1Δ* (GPc)
219 cross progeny for the trait at 21°C (**Methods**). We used this condition because the trait is less
220 genetically complex at 21°C than at higher temperatures, making it easier to find rough
221 segregants in a screen (LEE *et al.* 2016). The GPc screen produced a single rough segregant,
222 implying that expression of the rough phenotype in the absence of Flo8 and Sfl1 requires a
223 complex combination of alleles inherited from both BY and 3S.
224
225 *The three GPs vary in their potential to express the phenotype across temperatures*
226 Our GPb and GPc rough segregants were both obtained at 21°C, but were limited in their
227 abilities to express the phenotype at higher temperatures. Following from our previous work
228 showing that GPa segregants have the potential to express rough morphology across
229 temperatures (LEE *et al.* 2016), we assessed whether GPb and GPc strains also have the potential
230 to express the trait at higher temperatures. To check this, we backcrossed GPb and GPc F_2
231 segregants to both BY and 3S, and then phenotyped the resulting progeny at 21, 30, and 37°C
232 (**Figure 1F**). Note, such backcrossing generates new multi-locus genotypes that may have the
233 potential to express the rough phenotype at higher temperatures than the F_2 segregants recovered
234 from initial screens.
235

236 Upon examining 768 GPb and GPc backcross progeny at higher temperatures, we found that
237 some GPb backcross segregants expressed the trait at higher temperatures whereas GPc
238 backcross segregants did not (**Figure S1**). We observed varying degrees of temperature
239 sensitivity among the rough GPb segregants, with only a minority of rough individuals capable
240 of expressing the trait at 30 and 37°C (**Figure S1**). These results suggest that the trait has a
241 greater genetic complexity among GPb segregants that express it across temperatures than
242 among GPb segregants that only express it at low temperature. They also show that GPc provides
243 an inherently limited potential for trait expression across temperatures, perhaps because Flo8 and
244 Sfl1 are necessary for expression of the trait at higher temperatures.
245
246 *The GPs uncover distinct loci*
247 To map loci involved in expression of the rough phenotype across temperatures, we generated >
248 60,000 and > 12,000 GPb and GPc backcross segregants, respectively. First-generation
249 backcross segregants were used exclusively in mapping, except in the case of the 3S backcross of
250 GPb at high temperature. Determining the genetic basis of the trait among GPb 3S backcross
251 segregants required combining information from the first-generation and second-generation
252 backcrosses (**Figure S2**). GPb segregants were phenotyped at 21, 30 and 37°C, while GPc
253 segregants were only phenotyped at 21°C. Low-coverage whole genome sequencing was
254 performed on between 48 and 151 individuals for each GP–backcross–temperature combination,
255 and loci associated with the trait were identified based on their enrichment among genotyped
256 segregants (**Methods**).
257
258 In past work, we identified eight loci that act in different multi-locus genotypes to enable GPa
259 segregants to express the trait at particular temperatures (**Figure 2**). BY and 3S contributed the
260 causal alleles at two and four of these loci, respectively, while the remaining two loci were
261 detected in both the BY and 3S states in different multi-locus genotype and temperature contexts
262 (**Figure 3A**). Here, genetic mapping focused on GPb segregants detected a total of 11 loci across
263 the three environments (**Figure 2**, **Figure S3**, **Table S1**). Among these loci, six and three were
264 detected in the BY and 3S allele states, respectively (**Figure 3A**). The other two loci were
265 identified in both the BY and 3S allele states. Eight of these loci influenced the trait's expression
266 independent of temperature. Of the remaining loci, two were detected among individuals that

267 could express the trait at up to 30°C, while the third was identified among individuals that could
268 express the trait at up to 37°C. In addition, we identified 12 loci in the presence of GPc (**Figure**
269 **2**, **Figure S3**, **Table S1**). Among the loci found in the presence of GPc, seven were contributed
270 by BY and five were contributed by 3S (**Figure 3A**).
271
272 Comparison of the loci detected in the presence of each of the three GPs revealed that 21 distinct
273 genomic regions were identified in total (**Figure 2**, **Table 1**, **Methods**). Among these loci, one
274 was found in the presence of all three GPs, 8 were found in the presence of two GPs, and 12
275 were found in the presence of a single GP. This indicates that nearly all of the detected loci show
276 differential responsiveness to the GPs and that the majority of the loci we have identified are
277 cryptic variants that only act in the presence of specific GPs.
278
279 *The GPs alter genotype-environment interaction*
280 We assessed how identified loci interact with particular GPs, each other, and temperature to
281 produce the rough phenotype. Our past work on GPa found that at particular levels of
282 temperature sensitivity, distinct sets of epistatic cryptic variants form multi-locus genotypes that
283 produce the phenotype (LEE *et al.* 2016). Although we could not analyze the GPc segregants in
284 the same manner, examination of GPb segregants produced results comparable to our findings
285 for GPa. Among GPb segregants expressing the trait exclusively at 21°C, we detected a pair of
286 interacting loci on chromosomes XIII and XV, which then allowed us to identify distinct multi-
287 locus genotypes present among these individuals (**Figure 3A**, **Figure S5**, **Note S1**, **Methods**).
288 Similar to our work on GPa (LEE *et al.* 2016), only one of the GPb multi-locus genotypes found
289 at 21°C provided a foundation upon which additional allele substitutions can facilitate trait
290 expression at higher temperatures (**Figure 3A**, black lines). Among these GPb segregants
291 exhibiting the trait at higher temperatures, single multi-locus genotypes indicative of higher-
292 order epistasis facilitated trait expression at temperatures up to 30 and 37°C (**Figure 3A**).
293 Comparison our results for GPb to our past work on GPa found that more than half of the loci
294 and the exact multi-locus genotypes differed between the two GPs (**Figure 3A**). These results
295 show that the GPs significantly modify genotype-environment interactions underlying the rough
296 phenotype.
297

298 *The GPs affect additivity and epistasis among identified loci*

299 The only temperature at which all three GPs enable trait expression is 21°C. To compare the
300 quantitative genetic architectures enabling the three GPs to induce the rough phenotype at this
301 temperature, we used allele and multi-locus genotype frequency data from backcrosses (**Figure**
302 **3B** through **3D**, **Methods**). If loci act in a predominantly additive manner in the presence of a
303 given GP, observed multi-locus genotype frequencies should match expected multi-locus
304 genotype frequencies. In contrast, if epistasis meaningfully contributes to the trait, observed
305 multi-locus genotype frequencies should depart from expected multi-locus genotype frequencies.
306 Based on these tests, we observed significant deviation from expected frequencies for GPa
307 (**Figure 3B**) and GPb (**Figure 3C**), confirming that epistasis plays a significant role in the trait in
308 the presence of these GPs. However, data for GPc suggested that trait expression in the presence
309 of this GP is entirely additive (**Figure 3D**). These findings imply that although the three GPs in
310 this study can each enable expression of the same rough phenotype, they do so not only through
311 largely distinct cryptic variants but also through fundamentally different quantitative genetic
312 architectures.

313

314 *Coding and regulatory variation in FLO11 plays an essential role in the trait*

315 Only a single locus exhibited a phenotypic effect in the presence of all three GPs. This locus
316 corresponds to the 3S allele of the *FLO11* coding region (LEE *et al.* 2016). The BY and 3S
317 alleles of *FLO11* possess not only 57 synonymous and 29 nonsynonymous SNP differences, but
318 also a length polymorphism of ~581 nucleotides (**Figure S6)**. $FLO11^{3S}$ encodes a longer cell-
319 surface protein than $FLO11^{BY}$, an attribute that is known to favor the expression of multi-cellular
320 traits like the rough phenotype (VERSTREPEN *et al.* 2005; FIDALGO *et al.* 2006; FIDALGO *et al.*
321 2008; ZARA *et al.* 2009; HOPE AND DUNHAM 2014; MATSUI *et al.* 2015). Although this length
322 polymorphism is likely causal for the trait, we cannot rule out the possibility that some of the
323 SNPs also play a role.

324

325 In addition to being a required component of GPb, we found the BY allele of the *FLO11*
326 promoter is necessary for GPc segregants to express the trait (**Figure 4A**, **Table 1**). *FLO11* has
327 one of the largest and most complex promoters in *S. cerevisiae*, with more than 17 transcription
328 factors and 6 signaling cascades capable of influencing its regulation (BRUCKNER AND MOSCH

329 2012). Through genetic engineering experiments, we localized the causal variant in the *FLO11*
330 promoter to a Rim101 binding site that is present in 3S but not BY (**Figure 4B, Figure 4C,**
331 **Figure S7**). This finding is consistent with the important role that transcriptional derepression of
332 *FLO11* plays in expression of the rough phenotype (TAYLOR AND EHRENREICH 2015b; TAYLOR
333 *et al.* 2016). We note that although Rim101 has been described as a *FLO11* activator in other
334 strains of *S. cerevisiae*, this role is indirect and mediated through its role in silencing *NRG1*
335 (KUCHIN *et al.* 2002; LAMB AND MITCHELL 2003; BARRALES *et al.* 2008), which encodes a
336 repressor that directly binds the *FLO11* promoter. The Rim101 binding site in the 3S *FLO11*
337 promoter most likely results in direct repression of *FLO11* by Rim101, which reinforces Sfl1-
338 mediated repression. These findings not only speak to the critical role of Flo11 in expression of
339 the rough phenotype in the BYx3S cross, but also illustrate how regulation of this gene by
340 multiple pathways determines the phenotypic effects of cryptic variation.
341
342 *GPa and GPb rough segregants utilize different sub-pathways that impact Ras*
343 Excluding the *FLO11* coding region and promoter, all remaining loci act in the presence of only
344 one or two of the GPs. To better understand the highly contextual effects of these cryptic
345 variants, we attempted to resolve detected loci to specific genes. Seven of the GPb-responsive
346 loci detected in this study were previously found to interact with either GPa or other GPs in
347 previous papers, in which they were mapped to individual genes (LEE *et al.* 2016; TAYLOR *et al.*
348 2016) (**Table 1**). These genes encode Ras-regulated transcription factors (*FLO8*, *MSS11*, *MGA1*,
349 *SFL1*), a protein kinase A subunit (*TPK3*), a TOR pathway component (*MDS3)*, and *IRA2*. Two
350 of the loci found in the current study among GPb segregants were located on chromosomes II
351 and XIV, and had never been detected in our past work (**Figure 2, Table 1**). Through genetic
352 engineering experiments, we resolved the chromosome XIV locus to *SRV2* (**Figure S8)**, which
353 encodes a post-translational activator of adenylate cyclase. At the chromosome II locus, the most
354 likely candidate is *SRB6*, which encodes an essential subunit of the RNA polymerase II mediator
355 complex. Previously, we showed that mutations disrupting other mediator components, Srb10
356 and Srb11 (also known as Ssn3 and Ssn8, respectively), can induce the rough phenotype by
357 interacting with a subset of the alleles that have a phenotypic effect in the presence of GPa
358 (TAYLOR *et al.* 2016) (**Note S2**).
359

360 Although loci interacting with GPa and GPb primarily act through the Ras pathway and many
361 loci interact with both GPs, some are specific to one or the other. Among these are *TRR1* and
362 *END3*, which were detected in GPa segregants but not GPb segregants, as well as *MDS3*, *SRV2*,
363 and *TPK3*, which were identified in GPb segregants but not GPa segregants. Notably, these
364 genes play a role in activating the Ras pathway through oxidative stress and actin organization
365 (**Figure 5**). Actin cytoskeleton stability is required for cell polarity and yeast-adhesion traits, and
366 is regulated in part by the effects of End3 and Srv2 on Ras signaling (DU AND AYSCOUGH 2009).
367 This process results in increased production of reactive oxygen species (ROS) through the
368 activity of Tpk3 (GOURLAY AND AYSCOUGH 2006). ROS accumulation is then influenced by
369 Trr1 (CHARIZANIS *et al.* 1999) and the TOR pathway, of which Mds3 is a component. Together,
370 Mds3, Srv2, and Tpk3 form a well-described sub-pathway that influences Ras activity
371 (GOURLAY AND AYSCOUGH 2006; DU AND AYSCOUGH 2009). Thus, although different loci cause
372 the trait in the presence of GPa and GPb, they appear to reflect different sub-pathways affecting
373 the same cellular processes, which ultimately impact how Ras-regulated transcription factors
374 influence *FLO11* activity.
375
376 *Cryptic variation in several pathways underlies the phenotype in GPc segregants*
377 Lastly, we sought to determine the genes harboring cryptic variants that interact with GPc.
378 Regarding GPc, 3 of the 10 identified loci also interact with either GPa or b. These loci
379 correspond to *END3*, *IRA2*, and a locus on chromosome XII. For chromosome XII and the
380 remaining seven loci, we identified likely candidate genes based on our highly resolved genetic
381 mapping data and publicly available research on these genes' functions and phenotypic effects.
382 One of these loci corresponds to *IRA1*, a Ras negative regulator and paralog of *IRA2* (LEE *et al.*
383 2016) (**Table 1**). To obtain additional support for the remaining candidate genes, we deleted
384 them from GPc rough segregants and determined whether their loss affected the colony trait. All
385 seven knockouts had an effect, suggesting genetic variation in these genes plays a causal role in
386 the rough phenotype (**Figure S9**).
387
388 Detection of *END3*, *IRA1*, and *IRA2* in the absence of Flo8 and Sfl1 indicates that Ras still
389 contributes to *FLO11* regulation in the absence of these transcription factors, possibly by
390 impacting the activities of other transcription factors (ESTRUCH 2000). The remaining loci

391 implicate alternative signaling pathways as being responsible for trait expression in GPc
392 segregants. The genes we identified in the other intervals were a TOR pathway gene and *MDS3*
393 paralog (*PMD1*), components of the MAP kinase (MAPK) signaling cascade (*DIG1*, *GPA1*)
394 (METODIEV *et al.* 2002), an environmentally-responsive transcriptional activator (*GCN4),* a Rab
395 GTPase that influences Ras (COSTANZO *et al.* 2010), MAPK (COSTANZO *et al.* 2016), and
396 Rim101 (ZHENG *et al.* 2010) signaling *(YPT6),* a stress responsive guanine exchange factor
397 (*SDC25*), and an enzyme that post-translationally modifies proteins to help them anchor into the
398 cell wall (*GPI8*). Of particular note for *GPA1*, the BY strain is known to carry a lab-derived
399 allele that is an expression QTL hotspot (YVERT *et al.* 2003), supporting the possibility that
400 *GPA1* allele state might also impact expression of the rough phenotype in the presence of GPc.
401 Additionally, $GPA1^{BY}$ was previously shown to influence other *FLO11*-dependent traits through
402 its downstream transcriptional activator Ste12 (MATSUI *et al.* 2015). Nearly all of the genes
403 identified in rough GPc segregants have the potential to directly or indirectly influence *FLO11*
404 transcription. The lone exception is *GPI8*, which could still influence Flo11 at the protein level,
405 as it is responsible for adding glycosylphosphatidylinositol (GPI) anchors to new proteins and
406 could affect Flo11's binding to the cell surface (BENGHEZAL *et al.* 1996). These results show the
407 abundant cryptic variation that exists within the *FLO11* gene regulatory network.
408
409 **Discussion**
410 We have detailed how different genetic perturbations can reveal distinct cryptic variants, thereby
411 enabling a multitude of genotype, environment, and phenotype relationships to produce the same
412 trait. Across the 21 loci that can contribute to the rough phenotype in the presence of GPa, GPb,
413 and GPc, all but one of them show phenotypic effects that depend on the GP that is present. This
414 single locus corresponds to the coding region of *FLO11*, supporting the notion that regulation of
415 Flo11 levels and stability is the central determinant of the rough phenotype's expression across
416 GPs, combinations of segregating loci, and temperature.
417
418 Bolstering the importance of variability in *FLO11* regulation to our findings, nearly all of the loci
419 that exhibit phenotypic effects influence *FLO11* in *trans.* Moreover, many of these loci are only
420 visible in the absence of a repressive Rim101 binding site in the *FLO11* promoter. These results
421 highlight the potentially important role that *cis*-regulatory polymorphisms can play in enabling

422 *trans*-regulatory polymorphisms to exert phenotypic effects. Indeed, *cis*-regulatory
423 polymorphisms have been shown to modify the effects of *trans* variants in other systems (REDDY
424 *et al.* 2012; WONG *et al.* 2017), thereby altering how genetic differences impact traits (PAYNE
425 AND WAGNER 2014). More generally, our findings imply that changes at the level of an
426 organismal phenotype—the rough colony trait—reflect complex genetic and environmental
427 effects on a key gene's regulatory network, here *FLO11*.
428
429 In addition to showing that different GPs enable distinct cryptic variants to have phenotypic
430 effects, we also demonstrate that the GPs modify how genotype-environment interactions impact
431 the trait. For both GPa and GPb, we find that certain combinations of epistatic alleles both enable
432 expression of the trait at a permissive temperature of 21°C, as well as provide the genetic
433 potential for the phenotype at higher temperatures. However, different loci and multi-locus
434 genotypes enable GPa and GPb segregants to express the trait at higher temperatures. In contrast,
435 GPc individuals are unable to express the phenotype at temperatures above 21°C, implying their
436 potential to express the trait across environments is constrained. These findings support the
437 concept that not all genotypes specifying the same trait possess comparable phenotypic
438 robustness (WAGNER 2012; PAYNE *et al.* 2014; PFENNIG AND EHRENREICH 2014; SIEGAL AND
439 LEU 2014; EHRENREICH AND PFENNIG 2016). In the case of the rough phenotype, our genetic
440 mapping and genetic engineering results imply that differences in phenotypic robustness relate to
441 changes in signaling and transcription factor activity across multiple pathways and sub-pathways
442 influencing *FLO11*.
443
444 Furthermore, whereas the rough phenotype in GPa and GPb segregants involves complex
445 epistatic effects, we find no evidence for epistasis in GPc rough segregants. This implies that by
446 eliminating the main transcriptional regulators of *FLO11*, we not only uncovered a different set
447 of cryptic variants but also converted the trait's genetic architecture from mainly epistatic to
448 additive. Perhaps this additivity at the phenotypic level reflects the cumulative effect of multiple
449 pathways influencing *FLO11* expression at the molecular level. While the majority of the loci
450 that interact with GPa and GPb correspond to components of the Ras pathway, many of the loci
451 found in the presence of GPc are involved in other signaling pathways that may have
452 compensatory functions (**Figure 5**). This is consistent with the idea that eliminating Flo8 and

453 Sfl1 might enable other pathways to play a stronger role in expression of *FLO11* and the rough
454 colony phenotype.
455
456 Although not an explicit focus of the current manuscript, our results also provide valuable
457 insights into genetic background effects, the phenomenon in which GPs show different
458 phenotypic effects in distinct individuals (NADEAU 2001; CHANDLER *et al.* 2013; EHRENREICH
459 2017). A number of recent studies have shown that these background effects often result from
460 higher-order epistasis between a GP and multiple segregating loci (CHANDLER *et al.* 2014;
461 TAYLOR AND EHRENREICH 2014; MIOTTO *et al.* 2015; TAYLOR AND EHRENREICH 2015b; LEE *et*
462 *al.* 2016; KUZMIN *et al.* 2018; MULLIS *et al.* 2018). Despite supporting an important role for
463 higher-order epistasis in background effects, our current work, in particular on GPc, also shows
464 that background effects can have much simpler underpinnings. In the context of GPc, identified
465 loci each show pairwise epistasis with the GP, but exhibit no epistasis with each other and thus
466 appear to act additively. These differences in quantitative genetic architecture again tie back to
467 differences in *FLO11* regulation, consistent with theoretical work suggesting that how GPs
468 perturb gene regulatory networks can impact whether loci show additive or epistatic effects
469 (GJUVSLAND *et al.* 2007).
470
471 In summary, our study demonstrates the large amount of cryptic variation that can underlie a
472 single phenotype and strongly implicates complex changes in transcription as a mechanism
473 regulating this cryptic variation. Our findings also illustrate how systematically characterizing
474 the impacts of GPs on genotype-environment-phenotype relationships can significantly advance
475 understanding of some of the most difficult, yet fundamental problems in complex trait genetics.
476
477 **Acknowledgments**
478 We thank Joseph Hale, Takeshi Matsui, Martin Mullis, Joann Phan, Rachel Schell, Fabian Seidl,
479 Matthew Taylor, and Gleidson Teixeira for valuable input regarding this project or manuscript.
480 The work reported in this paper was supported by grant R01GM110255 from the National
481 Institutes of Health to I.M.E, a fellowship from the Alfred P. Sloan Foundation to I.M.E, and a
482 fellowship from the São Paulo Research Foundation to A.L.V.C.

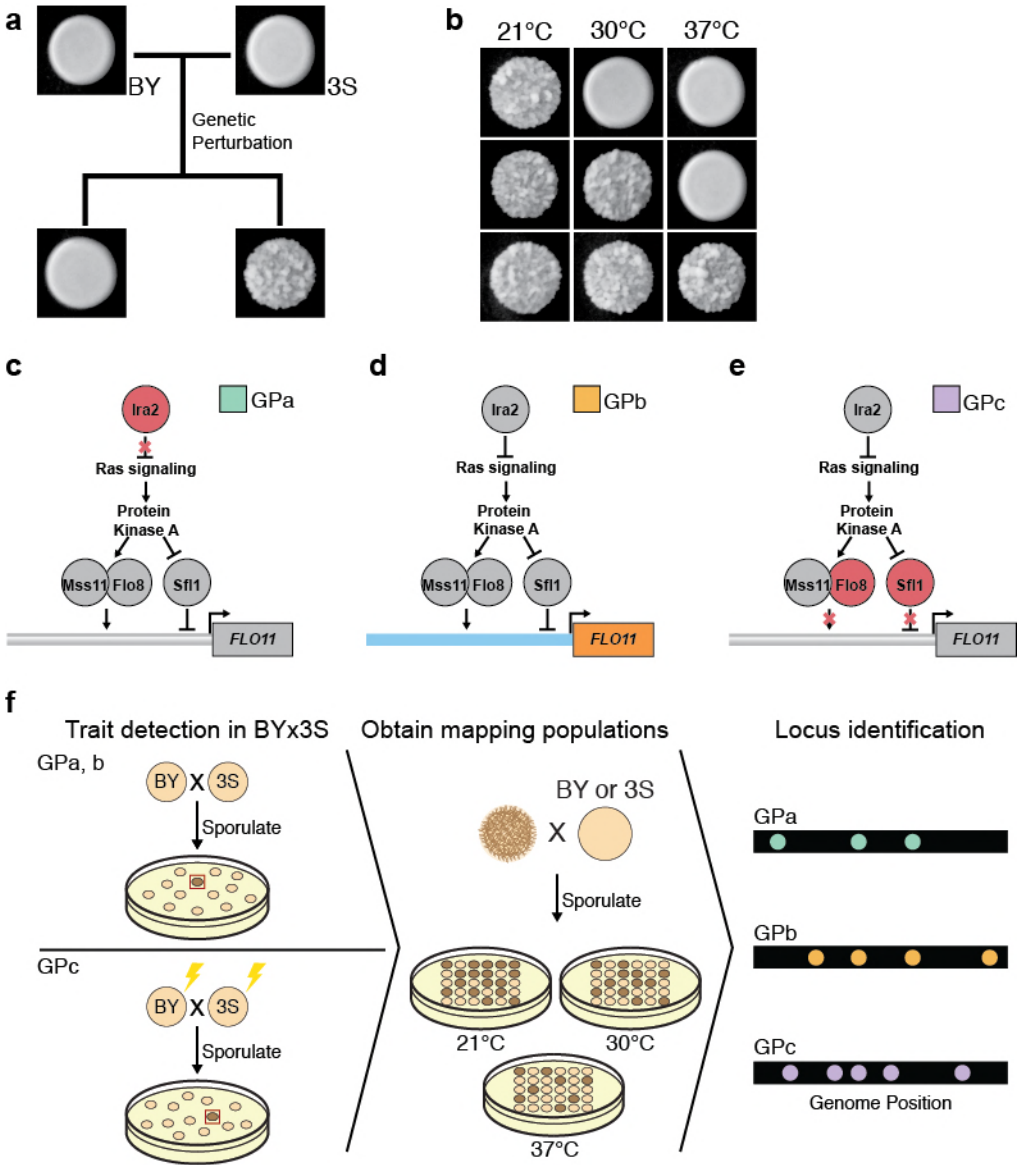

Figure 1: Different genetic perturbations ('GPs') interact with cryptic variation to cause rough morphology. (a) Certain GPs can cause BYx3S segregants to express a rough colony phenotype. **(b)** Expression of the colony trait can be temperature-sensitive, with individuals varying in their abilities to express the phenotype at 30 and 37°C. **(c)** GPa is a loss-of-function mutation in *IRA2*, which encodes a Ras negative regulator. **(d)** GPb results from recombination between the BY (blue) *FLO11* promoter and 3S (orange) *FLO11* coding region. **(e)** GPc is a double knockout of *FLO8* and *SFL1*, which encode the main Ras-dependent transcriptional regulators of *FLO11*. **(f)** GPa and GPb occurred spontaneously in the cross, while GPc was genetically engineered. Genetic mapping populations were generated using backcrossing, as well as screening for the trait at 21, 30, and 37°C. Loci associated with the trait were identified in

494 each backcross for each GP-temperature combination. Loci detected in the presence of GP were
495 then compared.

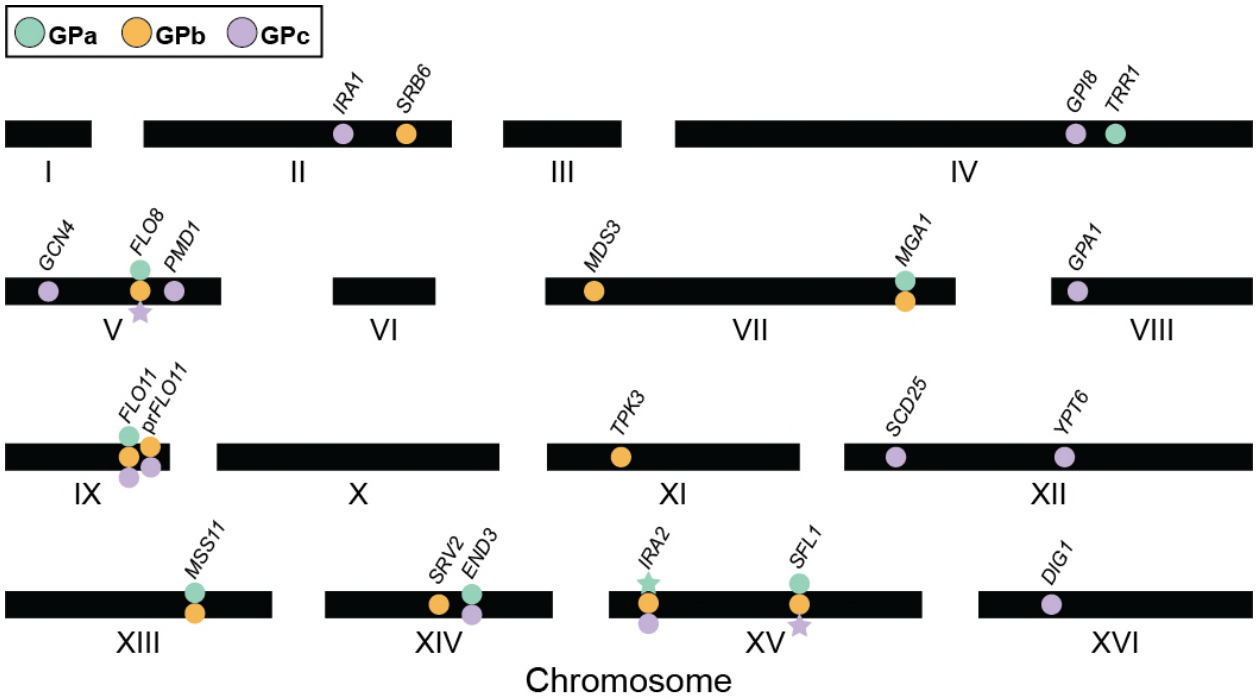

Figure 2: Loci identified in the presence of the GPs. Twenty-one loci were identified in total. Circles indicate cryptic variants, whereas stars indicate GPs.

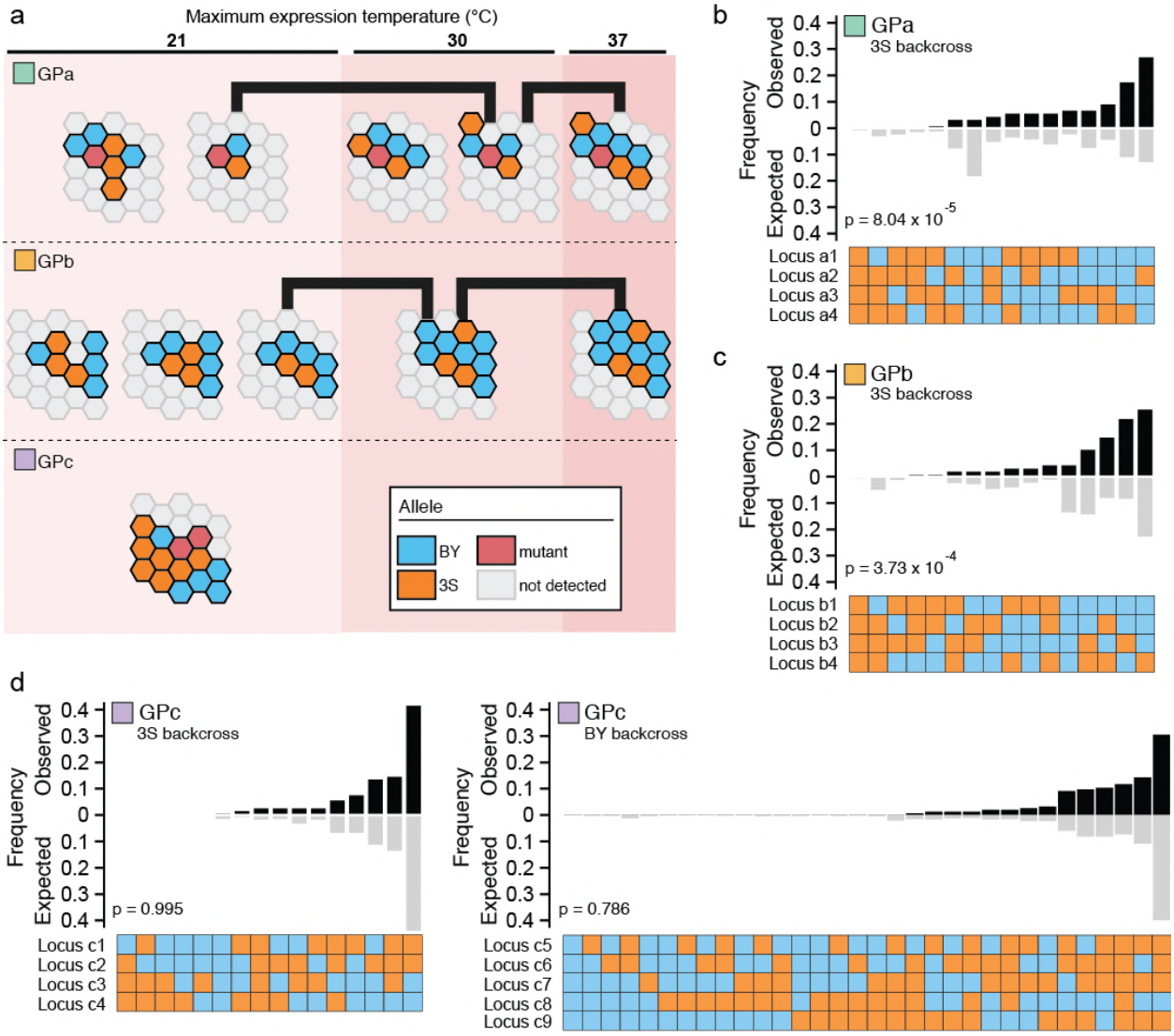

Figure 3: Loci detected across GPs and temperature sensitivity classes. (**a**) Loci interacting with GPa and GPb at 21 and 30°C act in different multi-locus genotypes. As shown with black lines, certain temperature-sensitive genotypes provide the potential for additional alleles to enable trait expression at higher temperatures. Loci interacting with GPc only have effects at 21°C. **(b)** For GPa individuals expressing the trait at only 21°C, observed multi-locus genotype frequencies at the four loci segregating in the 3S backcross do not reflect expected frequencies. This can occur if certain alleles exhibit epistasis and co-segregate in a non-random manner. **(c)** Observed and expected genotype frequencies based on four loci in GPb individuals expressing the trait at only 21°C. **(d)** Observed genotype frequencies in GPc individuals closely match expected frequencies, suggesting involved loci act in an additive manner.

511

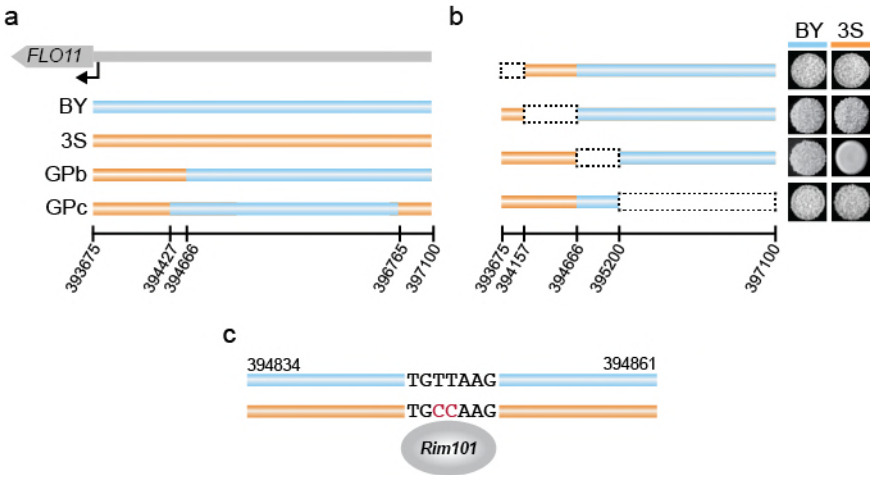

512

513 **Figure 4: A transcription factor binding site polymorphism is required for GPb and GPc**
514 **rough segregants to express the trait. (a)** The GPb and GPc *FLO11* promoters contain portions
515 of both the BY (blue) and 3S (orange) versions. **(b)** Genetic engineering experiments identified a
516 534 nucleotide segment of the BY-derived promoter as being responsible for the trait. **(c)** A
517 Rim101 transcription factor binding site that is absent in BY was found to be the causal
518 polymorphism.

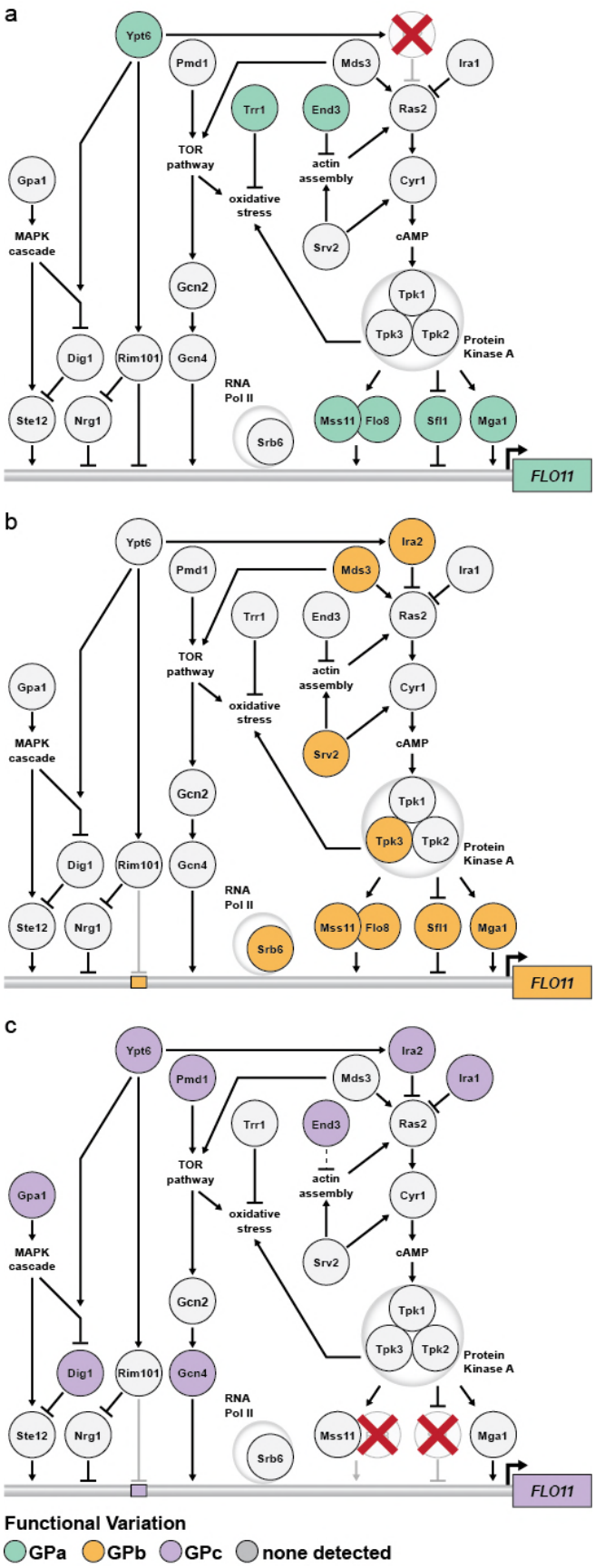
a
Ypt6
Pmd1
Mds3
Ira1
Trr1
End3
Ras2
TOR
pathway
actin
assembly
Gpa1
oxidative
stress
Cyr1
MAPK
cascade
Srv2
cAMP
Gcn2
Tpk1
Tpk3
Tpk2
Protein
Kinase A
Dig1
Rim101
Gcn4
RNA
Pol II
Ste12
Nrg1
Srb6
Mss11
Flo8
Sfl1
Mga1
FLO11
b
Ira2
c
Functional Variation
GPa
GPb
GPc
none detected

519

520 **Figure 5: GPs unmask cryptic genetic variation in parallel signaling pathways and sub-**
521 **pathways. (a)** Loci that interact with GPa influence *FLO11* regulation by the Ras pathway. **(b)**
522 GPb uncovers loci that primarily act through a different Ras sub-pathway involving Mds3, Srv2,
523 and Tpk3. **(c)** Loci interacting with GPc function in a number of different pathways that are
524 capable of regulating *FLO11* activity. The locations of transcription factor binding sites are not
525 intended to reflect specific positioning along the *FLO11* promoter.

526 **Table 1: Causal genes underlying identified loci**

Genetic Perturbation	Chr.	Gene	Function	Allele	Initial detection
GPc	2	*IRA1*	Ras negative regulator, *IRA2* paralog	3S	Taylor et al., 2016
GPb	2	*SRB6**	RNA Pol II subunit	BY	this paper
GPc	4	*GPI8*	GPI transamidase complex subunit	3S	this paper
GPa	4	*TRR1*	redox state regulator	3S	Taylor and Ehrenreich, 2014
GPc	5	*GCN4*	stress response transcription factor	3S	this paper
GPa,b	5	*FLO8*	Ras activated transcription factor	3S	Taylor and Ehrenreich, 2014
GPc	5	*PMD1*	growth regulator; *MDS3* paralog	BY	this paper
GPb	7	*MDS3*	TOR pathway growth regulator	3S	Taylor et al., 2016
GPa,b	7	*MGA1*	transcriptional activator	BY	Taylor and Ehrenreich, 2015
GPc	8	*GPA1*	G-protein	BY	this paper
GPa,b,c	9	*FLO11*	cell surfaace glycoprotein	3S	Lee et al., 2016
GPb,c	9	*prFLO11*	*FLO11* promoter	BY/3S	Taylor et al., 2016
GPb	11	*TPK3*	Protein Kinase A subunit	BY	Taylor et al., 2016
GPc	12	*SDC25*	Ras GEF	BY	this paper
GPa,c	12	*YPT6*	Rab GTPase	3S	Lee et al., 2016
GPa,b	13	*MSS11*	Ras activated transcription factor	BY	Taylor and Ehrenreich, 2014
GPb	14	*SRV2*	activator of adenylate cyclase	BY	this paper
GPa,c	14	*END3*	cell wall morphogenesis	BY, 3S	Taylor and Ehrenreich, 2014
GPb,c	15	*IRA2*	Ras negative regulator	BY	Taylor et al., 2016
GPa,b	15	*SFL1*	Ras inactivated transcription factor	BY	Taylor and Ehrenreich, 2015
GPc	16	*DIG1*	MAPK-regulated transcription factor	3S	this paper

527 * candidate gene

528 **References**

529 Atwell, S., Y. S. Huang, B. J. Vilhjalmsson, G. Willems, M. Horton *et al.*, 2010 Genome-wide
530 association study of 107 phenotypes in Arabidopsis thaliana inbred lines. Nature 465**:**
531 627-631.

532 Aylor, D. L., W. Valdar, W. Foulds-Mathes, R. J. Buus, R. A. Verdugo *et al.*, 2011 Genetic
533 analysis of complex traits in the emerging Collaborative Cross. Genome Res 21**:** 1213-
534 1222.

535 Barrales, R. R., J. Jimenez and J. I. Ibeas, 2008 Identification of novel activation mechanisms for
536 FLO11 regulation in Saccharomyces cerevisiae. Genetics 178**:** 145-156.

537 Benghezal, M., A. Benachour, S. Rusconi, M. Aebi and A. Conzelmann, 1996 Yeast Gpi8p is
538 essential for GPI anchor attachment onto proteins. EMBO J 15**:** 6575-6583.

539 Benjamini, Y., and Y. Hochberg, 1995 Controlling the false discovery rate: a practical and
540 powerful approach to multiple testing. Journal of the Royal Statistical Society, Series B
541 57**:** 289-300.

542 Bergman, A., and M. L. Siegal, 2003 Evolutionary capacitance as a general feature of complex
543 gene networks. Nature 424**:** 549-552.

544 Bloom, J. S., I. M. Ehrenreich, W. T. Loo, T. L. Lite and L. Kruglyak, 2013 Finding the sources
545 of missing heritability in a yeast cross. Nature 494**:** 234-237.

546 Bruckner, S., and H. U. Mosch, 2012 Choosing the right lifestyle: adhesion and development in
547 Saccharomyces cerevisiae. FEMS Microbiol Rev 36**:** 25-58.

548 Chandler, C. H., S. Chari and I. Dworkin, 2013 Does your gene need a background check? How
549 genetic background impacts the analysis of mutations, genes, and evolution. Trends
550 Genet 29**:** 358-366.

551 Chandler, C. H., S. Chari, D. Tack and I. Dworkin, 2014 Causes and consequences of genetic
552 background effects illuminated by integrative genomic analysis. Genetics 196**:** 1321-
553 1336.

554 Charizanis, C., H. Juhnke, B. Krems and K. D. Entian, 1999 The oxidative stress response
555 mediated via Pos9/Skn7 is negatively regulated by the Ras/PKA pathway in
556 Saccharomyces cerevisiae. Mol Gen Genet 261**:** 740-752.

557 Costanzo, M., A. Baryshnikova, J. Bellay, Y. Kim, E. D. Spear *et al.*, 2010 The genetic
558 landscape of a cell. Science 327**:** 425-431.

559 Costanzo, M., B. VanderSluis, E. N. Koch, A. Baryshnikova, C. Pons *et al.*, 2016 A global
560 genetic interaction network maps a wiring diagram of cellular function. Science 353.
561 Du, W., and K. R. Ayscough, 2009 Methyl beta-cyclodextrin reduces accumulation of reactive
562 oxygen species and cell death in yeast. Free Radic Biol Med 46: 1478-1487.
563 Dworkin, I., A. Palsson, K. Birdsall and G. Gibson, 2003 Evidence that Egfr contributes to
564 cryptic genetic variation for photoreceptor determination in natural populations of
565 Drosophila melanogaster. Curr Biol 13: 1888-1893.
566 Ehrenreich, I. M., 2017 Epistasis: Searching for Interacting Genetic Variants Using Crosses.
567 Genetics 206: 531-535.
568 Ehrenreich, I. M., and D. W. Pfennig, 2016 Genetic assimilation: a review of its potential
569 proximate causes and evolutionary consequences. Ann Bot 117: 769-779.
570 Estruch, F., 2000 Stress-controlled transcription factors, stress-induced genes and stress tolerance
571 in budding yeast. FEMS Microbiol Rev 24: 469-486.
572 Fidalgo, M., R. R. Barrales, J. I. Ibeas and J. Jimenez, 2006 Adaptive evolution by mutations in
573 the FLO11 gene. Proc Natl Acad Sci U S A 103: 11228-11233.
574 Fidalgo, M., R. R. Barrales and J. Jimenez, 2008 Coding repeat instability in the FLO11 gene of
575 Saccharomyces yeasts. Yeast 25: 879-889.
576 Geiler-Samerotte, K. A., Y. O. Zhu, B. E. Goulet, D. W. Hall and M. L. Siegal, 2016 Selection
577 Transforms the Landscape of Genetic Variation Interacting with Hsp90. PLoS Biol 14:
578 e2000465.
579 Gibson, G., and I. Dworkin, 2004 Uncovering cryptic genetic variation. Nat Rev Genet 5: 681-
580 690.
581 Gietz, R. D., and R. A. Woods, 2002 Transformation of yeast by lithium acetate/single-stranded
582 carrier DNA/polyethylene glycol method. Methods Enzymol 350: 87-96.
583 Gjuvsland, A. B., B. J. Hayes, S. W. Omholt and O. Carlborg, 2007 Statistical epistasis is a
584 generic feature of gene regulatory networks. Genetics 175: 411-420.
585 Gourlay, C. W., and K. R. Ayscough, 2006 Actin-induced hyperactivation of the Ras signaling
586 pathway leads to apoptosis in Saccharomyces cerevisiae. Mol Cell Biol 26: 6487-6501.
587 Hope, E. A., and M. J. Dunham, 2014 Ploidy-regulated variation in biofilm-related phenotypes in
588 natural isolates of Saccharomyces cerevisiae. G3 (Bethesda) 4: 1773-1786.

589 Jarosz, D. F., and S. Lindquist, 2010 Hsp90 and environmental stress transform the adaptive
590 value of natural genetic variation. Science 330: 1820-1824.
591 Kuchin, S., V. K. Vyas and M. Carlson, 2002 Snf1 protein kinase and the repressors Nrg1 and
592 Nrg2 regulate FLO11, haploid invasive growth, and diploid pseudohyphal differentiation.
593 Mol Cell Biol 22: 3994-4000.
594 Kuzmin, E., B. VanderSluis, W. Wang, G. Tan, R. Deshpande *et al.*, 2018 Systematic analysis of
595 complex genetic interactions. Science 360.
596 Lamb, T. M., and A. P. Mitchell, 2003 The transcription factor Rim101p governs ion tolerance
597 and cell differentiation by direct repression of the regulatory genes NRG1 and SMP1 in
598 Saccharomyces cerevisiae. Mol Cell Biol 23: 677-686.
599 Laughery, M. F., T. Hunter, A. Brown, J. Hoopes, T. Ostbye *et al.*, 2015 New vectors for simple
600 and streamlined CRISPR-Cas9 genome editing in Saccharomyces cerevisiae. Yeast 32:
601 711-720.
602 Le Rouzic, A., and O. Carlborg, 2008 Evolutionary potential of hidden genetic variation. Trends
603 Ecol Evol 23: 33-37.
604 Lee, J. T., M. B. Taylor, A. Shen and I. M. Ehrenreich, 2016 Multi-locus Genotypes Underlying
605 Temperature Sensitivity in a Mutationally Induced Trait. PLoS Genet 12: e1005929.
606 Li, H., and R. Durbin, 2009 Fast and accurate short read alignment with Burrows-Wheeler
607 transform. Bioinformatics 25: 1754-1760.
608 Li, H., B. Handsaker, A. Wysoker, T. Fennell, J. Ruan *et al.*, 2009 The Sequence
609 Alignment/Map format and SAMtools. Bioinformatics 25: 2078-2079.
610 Lo, W. S., and A. M. Dranginis, 1996 FLO11, a yeast gene related to the STA genes, encodes a
611 novel cell surface flocculin. J Bacteriol 178: 7144-7151.
612 Mackay, T. F., S. Richards, E. A. Stone, A. Barbadilla, J. F. Ayroles *et al.*, 2012 The Drosophila
613 melanogaster Genetic Reference Panel. Nature 482: 173-178.
614 Matsui, T., R. Linder, J. Phan, F. Seidl and I. M. Ehrenreich, 2015 Regulatory Rewiring in a
615 Cross Causes Extensive Genetic Heterogeneity. Genetics 201: 769-777.
616 McGuigan, K., and C. M. Sgro, 2009 Evolutionary consequences of cryptic genetic variation.
617 Trends Ecol Evol 24: 305-311.
618 Metodiev, M. V., D. Matheos, M. D. Rose and D. E. Stone, 2002 Regulation of MAPK function
619 by direct interaction with the mating-specific Galpha in yeast. Science 296: 1483-1486.

620 Miotto, O., R. Amato, E. A. Ashley, B. MacInnis, J. Almagro-Garcia *et al.*, 2015 Genetic
621 architecture of artemisinin-resistant Plasmodium falciparum. Nat Genet 47**:** 226-234.
622 Mullis, M. N., T. Matsui, R. Schell, R. Foree and I. M. Ehrenreich, 2018 The complex
623 underpinnings of genetic background effects. Nat Commun 9**:** 3548.
624 Nadeau, J. H., 2001 Modifier genes in mice and humans. Nat Rev Genet 2**:** 165-174.
625 Paaby, A. B., and M. V. Rockman, 2014 Cryptic genetic variation: evolution's hidden substrate.
626 Nat Rev Genet 15**:** 247-258.
627 Payne, J. L., J. H. Moore and A. Wagner, 2014 Robustness, evolvability, and the logic of genetic
628 regulation. Artif Life 20**:** 111-126.
629 Payne, J. L., and A. Wagner, 2014 The robustness and evolvability of transcription factor
630 binding sites. Science 343**:** 875-877.
631 Pfennig, D. W., and I. M. Ehrenreich, 2014 Towards a gene regulatory network perspective on
632 phenotypic plasticity, genetic accommodation and genetic assimilation. Mol Ecol 23**:**
633 4438-4440.
634 Queitsch, C., T. A. Sangster and S. Lindquist, 2002 Hsp90 as a capacitor of phenotypic variation.
635 Nature 417**:** 618-624.
636 Reddy, T. E., J. Gertz, F. Pauli, K. S. Kucera, K. E. Varley *et al.*, 2012 Effects of sequence
637 variation on differential allelic transcription factor occupancy and gene expression.
638 Genome Res 22**:** 860-869.
639 Rutherford, S. L., and S. Lindquist, 1998 Hsp90 as a capacitor for morphological evolution.
640 Nature 396**:** 336-342.
641 Seabold, S., and J. Perktold, 2010 Statsmodels: econometric and statistical modeling with
642 Python. Proc of the 9th Python in Science Conf**:** 57-61.
643 Siegal, M. L., and J. Y. Leu, 2014 On the Nature and Evolutionary Impact of Phenotypic
644 Robustness Mechanisms. Annu Rev Ecol Evol Syst 45**:** 496-517.
645 Taylor, M. B., and I. M. Ehrenreich, 2014 Genetic interactions involving five or more genes
646 contribute to a complex trait in yeast. PLoS Genet 10**:** e1004324.
647 Taylor, M. B., and I. M. Ehrenreich, 2015a Higher-order genetic interactions and their
648 contribution to complex traits. Trends Genet 31**:** 34-40.
649 Taylor, M. B., and I. M. Ehrenreich, 2015b Transcriptional Derepression Uncovers Cryptic
650 Higher-Order Genetic Interactions. PLoS Genet 11**:** e1005606.

651 Taylor, M. B., J. Phan, J. T. Lee, M. McCadden and I. M. Ehrenreich, 2016 Diverse genetic
652 architectures lead to the same cryptic phenotype in a yeast cross. Nat Commun 7**:** 11669.
653 Tong, A. H., M. Evangelista, A. B. Parsons, H. Xu, G. D. Bader *et al.*, 2001 Systematic genetic
654 analysis with ordered arrays of yeast deletion mutants. Science 294**:** 2364-2368.
655 Verstrepen, K. J., A. Jansen, F. Lewitter and G. R. Fink, 2005 Intragenic tandem repeats generate
656 functional variability. Nat Genet 37**:** 986-990.
657 Wach, A., A. Brachat, R. Pohlmann and P. Philippsen, 1994 New heterologous modules for
658 classical or PCR-based gene disruptions in Saccharomyces cerevisiae. Yeast 10**:** 1793-
659 1808.
660 Wagner, A., 2012 The role of robustness in phenotypic adaptation and innovation. Proc Biol Sci
661 279**:** 1249-1258.
662 Wong, E. S., B. M. Schmitt, A. Kazachenka, D. Thybert, A. Redmond *et al.*, 2017 Interplay of
663 cis and trans mechanisms driving transcription factor binding and gene expression
664 evolution. Nat Commun 8**:** 1092.
665 Yvert, G., R. B. Brem, J. Whittle, J. M. Akey, E. Foss *et al.*, 2003 Trans-acting regulatory
666 variation in Saccharomyces cerevisiae and the role of transcription factors. Nat Genet 35**:**
667 57-64.
668 Zara, G., S. Zara, C. Pinna, S. Marceddu and M. Budroni, 2009 FLO11 gene length and
669 transcriptional level affect biofilm-forming ability of wild flor strains of Saccharomyces
670 cerevisiae. Microbiology 155**:** 3838-3846.
671 Zheng, J., J. J. Benschop, M. Shales, P. Kemmeren, J. Greenblatt *et al.*, 2010 Epistatic
672 relationships reveal the functional organization of yeast transcription factors. Mol Syst
673 Biol 6**:** 420.
674

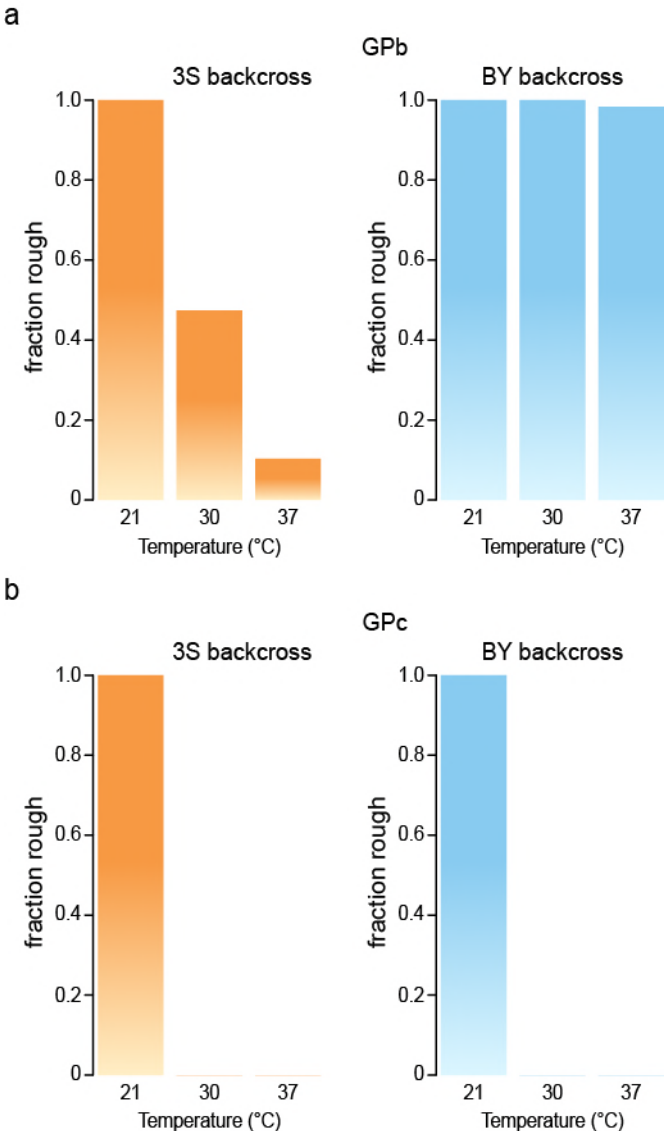

675
676 **Figure S1: GPb and GPc individuals differ in their temperature sensitivities. (a)** A subset of
677 GPb backcross segregants express rough morphology at 30 and 37°C. **(b)** GPc backcross
678 segregants are incapable of expressing the trait at 30 and 37°C. Ninety-six backcross segregants
679 were generated and phenotyped for each GP-backcross parent combination.

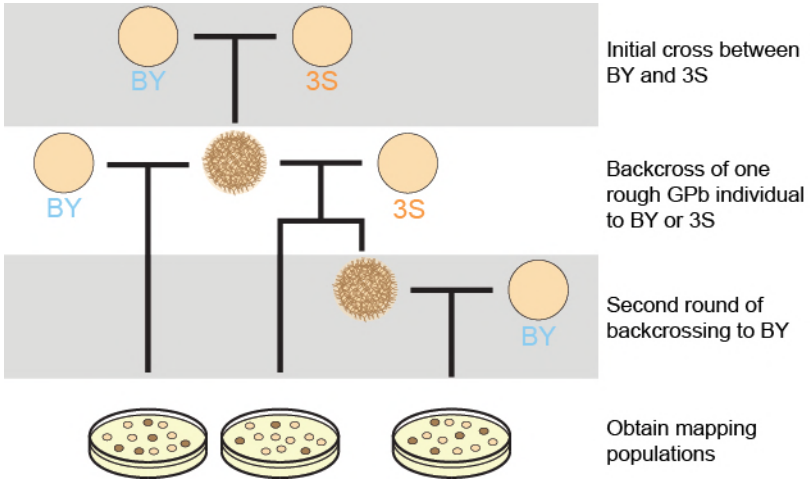

Figure S2: Scheme to generate GPb backcross mapping populations. A rough BYx3S F_2 segregant carrying GPb was backcrossed to BY and 3S. In the case of the cross to 3S, a second-generation backcross to BY was then performed, which was necessary to enrich for segregants that express the rough phenotype at 37°C.

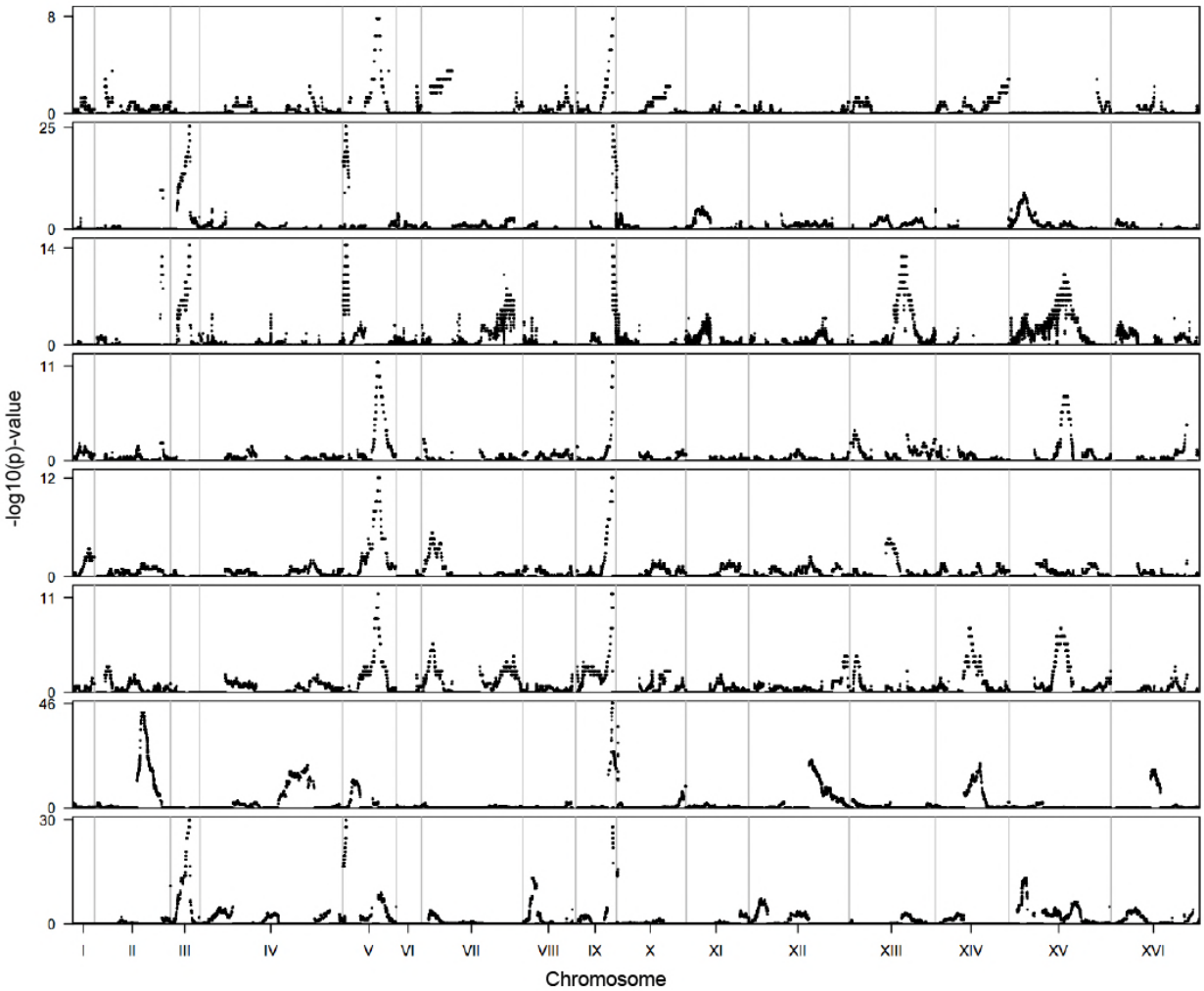

Figure S3: Genetic mapping for loci interacting with GPb and GPc. For each mapping population based on GP, backcross, and temperature sensitivity, a binomial test was performed for each SNP to identify regions of the genome associated with the rough phenotype. Results in are plotted in -$\log_{10}$(p)-values in the following order: GPb (BY backcross, 21, 30, 37°C), GPb (3S backcross, 21°C), GPb (3S backcross, 21, 30°C), GPb (2nd generation backcross, 21°C), GPb (2nd generation backcross, 21, 30°C), GPb (2nd generation backcross, 21, 30, 37°C), GPc (BY backcross, 21°C), GPc (3S backcross, 21°C).

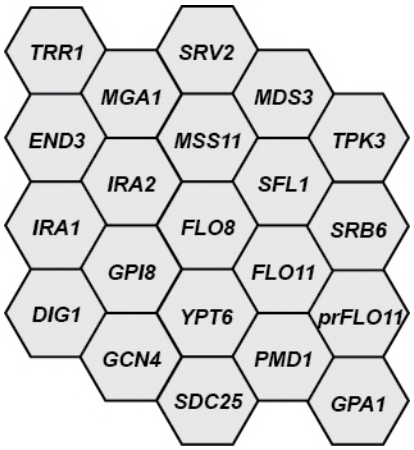

Figure S4: Key corresponding to gene position in Figure 3A.

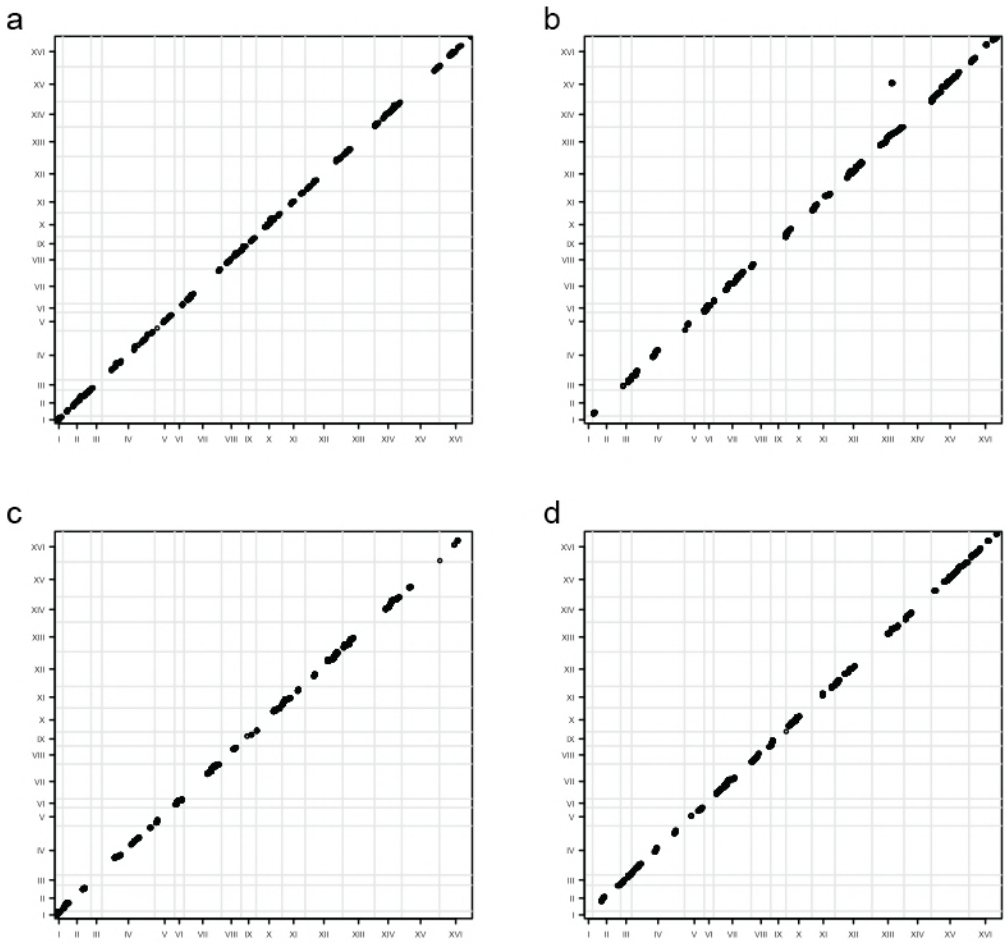

Figure S5: Scan for loci with correlated allele states. Significant p-values for χ^2 tests between each pair of uniquely segregating genomic regions: GPb – **(a)** backcross to BY, **(b)** backcross to 3S, and GPc – **(c)** backcross to BY, **(d)** backcross to 3S. Results are only plotted for the upper triangle. Significant results were only found in the GPb backcross to 3S.

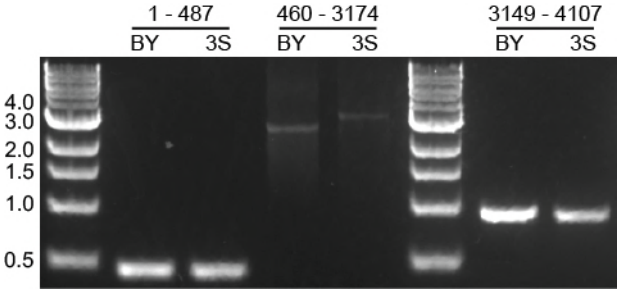

Figure S6: Variation in the *FLO11* coding region. The 3S strain carries a longer *FLO11* allele relative to BY. This is due to a ~500-600 nucleotide length polymorphism in the middle of the gene. Nucleotide positions are provided based on the BY gene sequence.

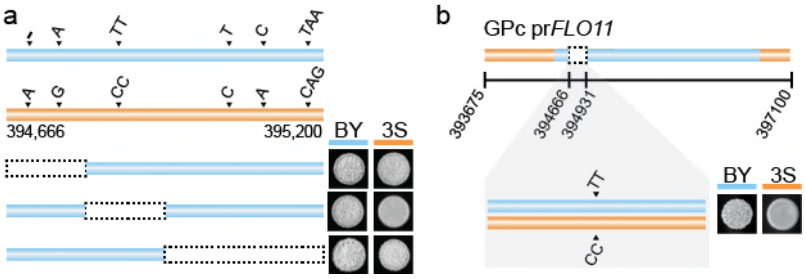

Figure S7: Additional pr*FLO11* fine mapping details. (a) Engineering of the six polymorphisms within the promoter region shown in Figure 3B revealed that replacement of a TT BY sequence at position 394,846 to 394,847 with the 3S CC allele ablates the phenotype. **(b)** Replacement of the same polymorphism in a strain with GPc also causes loss of the rough phenotype.

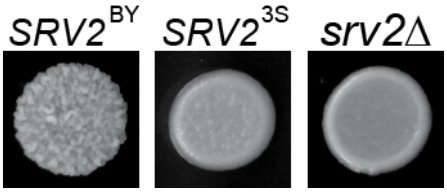

710

711 **Figure S8: The *SRV2* gene underlies a locus on chromosome XIV that interacts with GPb.**
712 Replacement of the BY *SRV2* allele with the 3S version results in loss of the rough phenotype. A
713 similar loss of phenotype is also observed when *SRV2* is deleted.

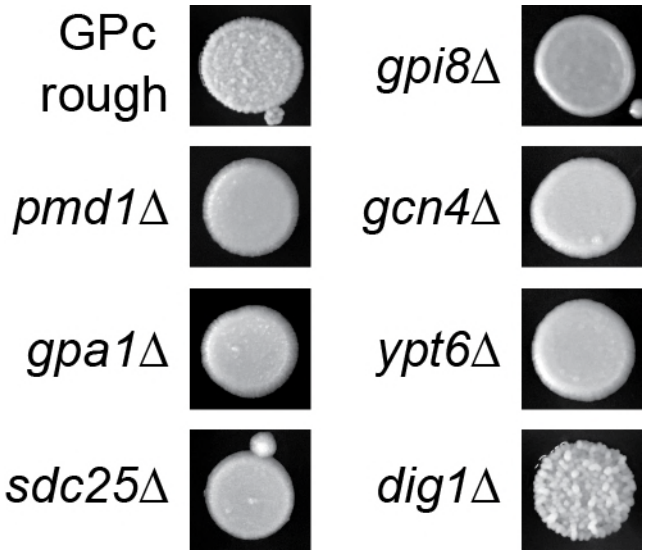

714

715 **Figure S9: Deletions support interactions between GPc and identified candidate genes.**
716 Complete deletion of the candidate genes in a GPc rough segregant was performed using tailed
717 *kanMX* cassettes. Deletion of six candidate genes causes loss of the phenotype. For the seventh
718 candidate gene, deletion enhances the phenotype. Notably, *DIG1* encodes a repressor of the
719 *FLO11* activator Ste12. Thus, the phenotypic enhancement seen upon its deletion is consistent
720 with cryptic variation promoting transcription of *FLO11*.

721

722 **Table S1: Loci detected across GPs and temperatures**

Genetic perturbation	Chromosome	Maximum temperature of trait expression	Allele	Upstream bound	Downstream bound	$-Log_{10}(p)$-value
b	2	21	BY	723181	734674	9.371
b	2	30	BY	705006	734674	10.706
b	2	37	BY	705006	734674	4.056
b	5	30	3S	368771	394911	10.709
b	5	37	3S	356220	383540	8.826
b	5	21, 30, 37	3S	353654	400481	6.665
b	7	30	3S	87038	214328	4.821
b	7	30	BY	894815	985698	6.917
b	7	37	3S	81381	143359	5.078
b	7	37	BY	852002	1000433	4.374
b	9	21	BY	396020	400489	8.101
b	9	21	BY	396027	439742	14.214
b	9	30	3S	386815	394651	10.709
b	9	30	BY	395106	416603	11.929
b	9	37	3S	386817	394001	10.127
b	9	37	BY	395106	396891	6.92
b	9	21, 30, 37	3S	386511	394651	6.665
b	11	21	BY	97364	242623	4.898
b	11	21	BY	97394	243150	5.854
b	11	30	BY	154545	257237	3.703
b	13	21	BY	319105	924189	4.898
b	13	21	BY	395951	664756	5.854
b	13	21	BY	570969	605817	14.214
b	13	30	BY	548950	609784	10.706
b	13	37	BY	554372	923918	4.98
b	14	37	BY	356409	394076	7.711
b	15	21	BY	100250	202290	4.18
b	15	21	BY	111105	223620	4.283
b	15	21	BY	129314	193871	8.708
b	15	21	BY	553016	631585	4.853
b	15	30	BY	131162	299083	3.703
b	15	30	BY	559403	628841	9.617
b	15	37	BY	498862	623604	6.731
c	2	21	3S	503310	531496	40.859
c	4	21	3S	961848	1151234	16.42

c	5	21	3S	105743	16630	11.564
c	5	21	BY	377154	438640	8.564
c	8	21	BY	98357	122190	13.319
c	9	21	3S	387502	394427	44.464
c	9	21	BY	395106	397560	26.391
c	12	21	BY	109399	173876	6.429
c	12	21	3S	642815	680926	20.06
c	14	21	BY	445983	473648	17.815
c	15	21	BY	147945	182906	12.549
c	16	21	3S	429704	477416	16.42

724 **Note S1:** For GPb individuals expressing the rough phenotype at 21°C, we detected two multi-
725 locus genotypes among segregants from the backcross to 3S. We also identified a third genotype
726 in the second-generation backcross population, involving a different combination of alleles than
727 those from the initial 3S backcross.
728
729 **Note S2:** We deleted each non-essential gene at the GPb chromosome II locus – *RRT2*, *HIS7*,
730 *ARO4*, *MRPS5*, *MTC4*, *SHG1*, and *YBR259W* – and found that none of these deletions caused
731 loss of the rough phenotype. This implies that loss-of-function in a non-essential gene is not
732 responsible for the trait at this locus, and the causal genetic variant is either a gain-of-function
733 polymorphism or is an essential gene. Among the essential genes at this locus, *SRB6* was
734 determined to be the strongest candidate.